



Enhancing resin-dentin bond durability using a novel mussel-inspired monomer



Kang Li^a, Chenmin Yao^b, Yuhong Sun^c, Kun Wang^d, Xiangtao Wang^b, Zhengzhi Wang^d, James Kit Hon Tsoi^e, Cui Huang^{b, **}, Cynthia Kar Yung Yiu^{a, *}

^a Paediatric Dentistry and Orthodontics, Faculty of Dentistry, The University of Hong Kong, Prince Philip Dental Hospital, 34 Hospital Road, Sai Ying Pun, Hong Kong, 999077, China

^b The State Key Laboratory Breeding Base of Basic Science of Stomatology (Hubei-MOST) & Key Laboratory for Oral Biomedicine Ministry of Education, School and Hospital of Stomatology, Wuhan University, Wuhan, 430079, China

^c Center of Stomatology, Peking University Shenzhen Hospital, Shenzhen, 518036, China

^d Department of Engineering Mechanics, School of Civil Engineering, Wuhan University, Wuhan, 430072, China

^e Dental Materials Science, Applied Oral Sciences, Faculty of Dentistry, The University of Hong Kong, Prince Philip Dental Hospital, 34 Hospital Road, Sai Ying Pun, Hong Kong, 999077, China

ARTICLE INFO

Keywords:

Mussel
Monomer
Collagen
N-(3,4-dihydroxyphenethyl)methacrylamide
Bond durability
Resin-dentin interface

ABSTRACT

Numerous approaches have been developed to improve the resin-dentin bond performance, among which the bio-application of mussel-derived compounds have drawn great attention recently. To assess the performance of N-(3,4-dihydroxyphenethyl)methacrylamide (DMA), a mussel-derived compound, as a functional monomer in dental adhesive, its potential property to cross-link with dentin collagen and polymerize with adhesive will first be evaluated by transmission electron microscopy (TEM), attenuated total reflectance technique of Fourier transform infrared (ATR-FTIR), and atomic force microscopy (AFM) via Peakforce QNM mode. After validating the influence of DMA on collagen and adhesive separately, the overall performance of DMA/ethanol solution as a primer in dentin bonding was examined using micro-tensile bond strength (μ TBS) testing, fracture pattern observation, and nanoleakage evaluation both immediately and after 10,000 times thermocycling aging. The inhibitory effect of DMA on endogenous metalloproteinases (MMPs) was evaluated by *in situ* zymography using confocal laser scanning microscopy (CLSM) and the cytotoxicity of DMA was evaluated using cell counting kit-8. Results demonstrated that DMA successfully cross-linked with dentin collagen via non-covalent bonds and had no influence on the polymerization and mechanical properties of the adhesive. Furthermore, even after 10,000 times thermocycling aging, the μ TBS and nanoleakage expression of the DMA-treated groups showed no significant change compared with their immediate values. *In situ* zymography revealed reduced endogenous proteolytic activities after the application of DMA, and no cytotoxicity effect was observed for DMA concentration up to 25 μ mol/L. Thus, DMA could be used as a novel, biocompatible functional monomer in dentin bonding.

1. Introduction

The progress of resin-dentin bonding technique has greatly revolutionized today's dental practice, which has gradually replaced the traditional amalgam fillings to more aesthetic tooth-colored resin composite restorations [1,2]. The longevity of these tooth-colored restoration highly depends on the integrity of resin-dentin interface (aka Hybrid

layer), which is composed by the micro-interlocking of demineralized dentin collagen network with infiltrated adhesive monomers [3]. To facilitate the infiltration of adhesive monomers, the dentin surface has to be kept relatively moist to prevent the collapse of demineralized collagen fibrils [4]. However, even though the wet bonding technique has achieved a much higher resin-dentin bond strength compared with the previous dry bonding technique, the remnant water within dentin matrix

* Corresponding author. Paediatric Dentistry and Orthodontics, 2nd Floor, Prince Philip Dental Hospital, 34-Hospital Road, Sai Ying Pun, Hong Kong (SAR), China.

** Corresponding author. School and Hospital of Stomatology, Wuhan University, #237 Luoyu Road, Hongshan District, Wuhan, 430079, China.

E-mail addresses: likang@connect.hku.hk (K. Li), yao_chenmin@whu.edu.cn (C. Yao), sunyuhong1024@whu.edu.cn (Y. Sun), 2015301890001@whu.edu.cn (K. Wang), 2019283040033@whu.edu.cn (X. Wang), zhengzhi.wang@whu.edu.cn (Z. Wang), jkhtsoi@hku.hk (J.K.H. Tsoi), huangcui@whu.edu.cn (C. Huang), ckyyiu@hku.hk (C.K.Y. Yiu).

<https://doi.org/10.1016/j.mtbio.2021.100174>

Received 22 September 2021; Received in revised form 9 November 2021; Accepted 28 November 2021

Available online xxx

2590-0064/© 2021 Published by Elsevier Ltd. This is an open access article under the CC BY-NC-ND license (<http://creativecommons.org/licenses/by-nc-nd/4.0/>).

becomes the “ticking time bomb”, which could explode at any time [4,5]. First, the remnant water in demineralized dentin has resulted in a highly porous hybrid layer [6]. The interspaces at the bottom of the hybrid layer cannot be completely occupied by adhesive monomers, and the denuded demineralized collagen fibrils are therefore under great threat from water hydrolysis and protease degradation [7,8]. Second, the ester group (–CO–O–R–) in both acrylate- and methacrylate-based monomers, especially 2-hydroxyethyl methacrylate (HEMA), could be hydrolyzed by water over time, which is detrimental to the mechanical properties of the hybrid layer [9,10]. Consequently, resin-dentin bond durability remains a clinically significant challenge, leading to frequent replacement of the resin-based restorations at extra costs [11,12].

Even though several strategies (eg. ethanol wet bonding [13] and biomimetic remineralization [14]) have been proposed in recent years to change the water-rich environment of dentin matrix and modify the well-received “wet bonding” philosophy, the application steps of these methods are time-consuming and unpractical for chair-side use based on the published results [15,16]. Hence, there is a significant demand to find a novel material which could strengthen the mechanical properties of the resin-dentin interface under humid environment and remain hydrolytically stable *per se*.

Mussel is a small shellfish that spread world-widely in the marine environment. Because of its unique wet adhesion properties, the interaction between mussel plaques and substrate under humid environment has been extensively studied by the scientific community, providing fruitful perspectives for clinical applications [17–19]. In the harsh marine environment, the mussel plaque-rock interface is subjected to sudden shocks from turbulent currents in different directions, diurnal temperature changes, and protease degradation by secreted enzymes from attached microbes [17,20]. Similarly, with the daily activities happening in oral cavity, the resin-dentin interface is required to endure the repeated mechanical stress induced by chewing each day [21], therefore providing a stable bonded structure that can counter the hydrolysis threat from remnant water or saliva [3], withstand chemical interference from rapid changes in temperature and pH [22], and resist the proteolytic attack from endogenous matrix metalloproteinase (MMPs) is of paramount importance [23]. Consequently, several studies have tried to translate the wet adhesion property from mussel into dentin bonding treatment, with some acceptable results achieved *in vitro* [24, 25].

The extraordinary wet adhesion property of mussel is attributed to the L-3,4-dihydroxyphenylalanine (Dopa) residues in mussel adhesive protein (MAP), which contained the catechol group [17]. It has been reported that the catechol group of MAP could form strong binding force with collagen via hydrogen bond, cation- π and electrostatic interactions [26]. Besides, the catechol group could chelate with the Zn^{2+} and Ca^{2+} ions on the catalytic domain of MMPs, thus altering the 3D structure of protein and deviating the normal procedure of substrate degradation [27, 28]. In the study by Fang et al. [25], the MAP-treated dentin surface showed anti-proteolytic properties with positive outcomes on the durability of the resin-dentin interface. Nevertheless, we should be aware that the macromolecule proteins derived from mussel cannot polymerize with adhesive and are only simply mixed with the adhesive resins [25]. The long-term stability of mussel-derived proteins and whether they will gradually leach out from the hybrid and adhesive layers over time remain in doubt.

Consequently, in the current study, a potential mussel-inspired functional monomer, namely *N*-(3,4-dihydroxyphenethyl)methacrylamide (DMA) (CAS No. 471915-89-6) (Fig. 1), was selected and evaluated. Theoretical saying, the carbon-carbon double bond of DMA could polymerize with adhesive monomers, the catechol group could cross-link with dentin collagen and inhibit endogenous MMPs, while the amide bond is hydrolytically stable [29]. Therefore, the current study aims to evaluate the performance of DMA as a functional monomer in dental adhesive to enhance the durability of resin-dentin interface and

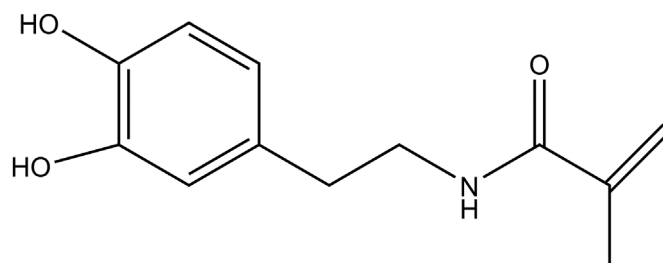


Fig. 1. The chemical structure of *N*-(3,4-dihydroxyphenethyl)methacrylamide (DMA).

inhibit endogenous MMPs. The null hypotheses tested in the current research are that the application of DMA (1) has no cross-linking effect with dentin collagen, (2) has no influence on the degree of conversion and mechanical properties of adhesive, (3) does not affect the bond strength and the quality of the resin-dentin interface after 24 h water storage and 10,000 times thermocycling, and (4) has no effect on the activity of endogenous MMPs.

2. Materials and methods

2.1. Tooth collection and experimental solutions preparation

Following the protocol (UW 19–240) approved by the local Institutional Review Board, in total 52 non-decayed, intact human third molars were taken after obtaining the informed consents from donors. The donated teeth were preserved in 0.1% thymol solution at 4 °C and used within one month of extraction.

The DMA utilized in the present work was purchased from Chem-Shuttle (Hayward, CA, USA), and was dissolved in the mixed solvent of ethyl alcohol (EtOH) and water in the volume ratio of 1:1. After water-bath heating at 37 °C for 30 min, three DMA-dissolved solutions were obtained: 1 mmol/L DMA-EtOH solution (1 mM DMA); 5 mmol/L DMA-EtOH solution (5 mM DMA); and 10 mmol/L DMA-EtOH solution (10 mM DMA). The 50% EtOH aqueous solution without DMA served as the Control group. The experimental solutions were stored in brown sample tubes under room temperature with the gap sealed by Parafilm® (Amcor, Zürich, Switzerland).

2.2. Cross-linking of DMA with type I collagen

The type I collagen from rat tail (Sigma-Aldrich, St Louis, Mo) was dissolved in 1% acetic acid solution at the concentration of 1 mg/mL. The 200-mesh carbon-coated Ni grids (T10022 N, Tianld Co., China) were placed over the collagen solution, and exposed to the ammonia vapor for 4 h, inducing the self-assembly of collagen fibrils [30]. The grids were then placed over the four different DMA-EtOH solutions for 60 min, respectively, and observed under transmission electron microscopy (TEM) (Hitachi HT7700-SS, Tokyo, Japan) at 80 kV.

2.3. Spectroscopic measurements on the interaction of DMA with dentin collagen

Four teeth were used for the attenuated total reflectance technique of Fourier transform infrared (ATR-FTIR) spectroscopy (Spectrum Two, Perkin-Elmer) evaluation. From each tooth, two 5 × 5 × 0.5 mm mid-coronal dentin slabs were obtained by cutting the coronal and root parts of the tooth using a low-speed diamond saw (Isomet, Buhler Ltd., Lake Bluff, IL, USA) under water cooling. The dentin slabs were demineralized by 10% phosphoric acid for 5 h to remove the apatite, and completely washed with deionized water. After treatment, the demineralized dentin slabs were allocated into four groups and placed in the four different DMA-EtOH solutions for 60 min, respectively, followed by

ATR-FTIR evaluation with 10 scans in the range of 4000–500 cm^{-1} with a resolution of 4.0 cm^{-1} .

2.4. Degree of conversion

Twenty microliter DMA-EtOH solution and 180 μL dental adhesive (Adper Single Bond 2, 3 M ESPE, St. Paul, MN, USA) was pipetted to a brown sample tube and fully oscillated for 30 s before test. To mimic the potential influence of remnant DMA on the polymerization of adhesive after dentin pretreatment, the DMA-EtOH solutions were mixed with the dental adhesive in the volume ratio of 1:9. One drop of mixed adhesive was spread on the top plate of ATR-FTIR, and polymerized for 20 s using a light-curing unit (Demi Plus, Kerr, Orange CA, USA) at approximately 600 mW/cm^2 radiation. After light-curing, another 100 s was waited for the post-polymerization of adhesive. The spectra of FTIR were obtained with 10 scans in the range of 1800–1500 cm^{-1} with a resolution of 4 cm^{-1} . The degree of conversion (DC) was calculated based on the following equation:

$$DC(\%) = 1 - \frac{\text{Cured} \left[\frac{\text{Abs}(1638)}{\text{Abs}(1608)} \right]}{\text{Uncured} \left[\frac{\text{Abs}(1638)}{\text{Abs}(1608)} \right]} \times 100\%$$

The Abs (1638) indicated the absorbance of the C=C stretching vibration at 1638 cm^{-1} , while Abs (1608) indicated the absorbance of the symmetric ring stretching at 1608 cm^{-1} which served as the internal standard. The average of six readings of each group after 20 s light curing and 100 s post-polymerization were obtained. Within each curing time, the Kruskal-Wallis test followed by Dunn-Bonferroni multiple comparison is selected, while within each group, the Mann-Whitney test is selected ($\alpha = 0.05$).

2.5. Peakforce QNM test by atomic force microscope

A schematic showing the dentin bonding procedures and subsequent evaluations is depicted in Fig. 2. Four teeth were sectioned under water cooling to remove the occlusal crown and expose the mid-coronal dentin surface. The dentin surface was wet-polished (600-grit SiC paper) for 1 min, etched with phosphoric acid (Scotchbond Universal Etchant, 3 M ESPE, St. Paul, MN, USA) for 15 s, thoroughly rinsed with water spray, and applied with one of the four DMA-EtOH solutions for 30 s twice, respectively. After gently air-blown for 3 s, two coats of Adper Single Bond 2 was rubbed on the dentin surface circularly followed by 20 s light-curing at approximately 600 mW/cm^2 radiation. Four 1-mm thick resin composite layers (Filtek Z350 XT, 3 M ESPE, St. Paul, MN, USA) were built up on the dentin and polymerized with 20 s for each layer. The compositions and the application methods for the etchant, adhesive and resin composite are summarized in Table 1.

After 24 h water storage at 37 °C, the bonded teeth were sectioned parallel to the long axis to yield three 1.5 mm thick resin-dentin slabs for each tooth. The produced resin-dentin slabs were wet-polished with SiC papers of 600, 1200, 2000, and 3000 grits, and further polished by an automatic polisher (EcoMet 250/AutoMet 250, Buehler) using diamond suspensions (9, 3, 1, 0.25, and 0.05 μm in sequence) (MetaDi, Buehler Ltd., Lake Bluff, IL, USA) after embedding the slabs into epoxy blocks [31]. All samples were stored in artificial saliva with 0.2% sodium azide to prevent microbial growth prior to test.

The measurement was conducted under the PeakForce QNM mode of atomic force microscopy (AFM) (MultiMode 8, Bruker) using the probe DNISP-HS ($k \sim 350 \text{ N/m}$ nominal, tip radius $< 40 \text{ nm}$). The scanning size for each area was 50 \times 50 μm^2 , and a digital resolution of 256 \times 256 datapoints (in total 65,536 datapoints) with a scanning rate at 0.5 Hz was adopted. Twenty different Regions Of Interests (ROI: adhesive, hybrid layer) with area of 1.96 \times 1.96 μm^2 (equals to 10 \times 10 = 100 datapoints) were randomly selected from each slab, and the average values of these

ROIs were calculated to represent the Derjaguin-Müller-Toporov (DMT) modulus of the adhesive and hybrid layers of each slab [32]. Three slabs from each group were tested in the same method and the average values were analyzed by one-way analysis of variance (ANOVA) followed by *post hoc* Tukey's test ($\alpha = 0.05$) after validating the normality and homogeneity of the data.

2.6. Micro-tensile bond strength (μTBS) test

Forty ($n = 10$ per experimental group) intact human third molars were prepared as the procedure described in Section 2.5 to yield 0.9 mm thick resin-dentin slabs. The middle resin-dentin slab from each tooth was stored for interfacial nanoleakage detection, while the remaining slabs were sectioned into resin-dentin beams with dimensions of 0.9 \times 0.9 \times 8 mm. After excluding the unqualified beams with existing enamel and lack of length for attachment onto the tester, six samples from each tooth were collected and randomly allocated to two subgroups ($n = 30$ for each subgroup), namely immediate group (only 24 h water storage at 37 °C) and aged group (10,000 times thermocycling, 5–55 °C, 15 s dwell time and 7 s transferring time). After the above treatment, the qualified samples were fixed on the μTBS tester (Model 4440, Instron Inc., Canton, MA), and was subjected to fracture at the cross-head speed of 1 mm/min. The μTBS value (MPa) of each specimen was calculated by dividing the force (N) by the surface area (mm^2). The result was analyzed by two-way ANOVA (Factors: DMA concentrations and aging) followed by *post hoc* Tukey's test ($\alpha = 0.05$) after validating the normality and homogeneity of the data.

2.7. Failure mode observation

The fractured samples after μTBS test were collected and observed under scanning electron microscopy (SEM) (SU-1510, Hitachi High-Technologies Corp., Tokyo, Japan), and their distribution of failure modes on dentin side was documented in five different categories following the method described by Li et al. [33]: (AD) adhesive failure; (CC) cohesive failure in composite; (CD) cohesive failure in dentin; (M1) the mixed failure of AD + CC; and (M2) the mixed failure of AD + CD. The failure modes of AD, CC and M1 indicate that the failure occurs at the upper part of the hybrid layer or composite with no dentin matrix exposed, which suggests the resin-dentin interface is strong enough to withstand the external breaking force. On the contrary, the failure modes of M2 and CD indicate that failure occurs at the bottom part of the hybrid layer with dentinal tubules and collagen network exposed, which suggests the integrity of resin-dentin interface is jeopardized. Therefore, the percentage of failure pattern in each group before and after aging was calculated, and the difference in the percentage between upper hybrid layer bond failure (CC + M1+AD) and bottom hybrid layer bond failure (M2+CD) was analyzed using Chi-Square test between the groups within each time point ($\alpha = 0.05$).

2.8. Nanoleakage evaluation

The saved middle resin-dentin slabs were randomly allocated to immediate group ($n = 5$) and thermocycling aged group ($n = 5$). After treatment, an approximately 1-mm width area around the resin-dentin interface was left unprotected, while the rest part of the slabs was brushed with nail varnish for two layers. The specimens were soaked into 50 wt% ammoniacal silver nitrate solution for 24 h, completely washed under running water for 5 min and transferred into a photo-developing solution, and each surface was exposed to fluorescence light irradiation for 6 h [34]. After treatment, the specimens were rough polished using a series of SiC paper with 600-, 1200-, 2000-, and 3000-grit, and then fine polished using 1 and 0.5 μm diamond powders. The specimens were then ultrasonically cleaned, dried, sputter-coated with gold and observed via

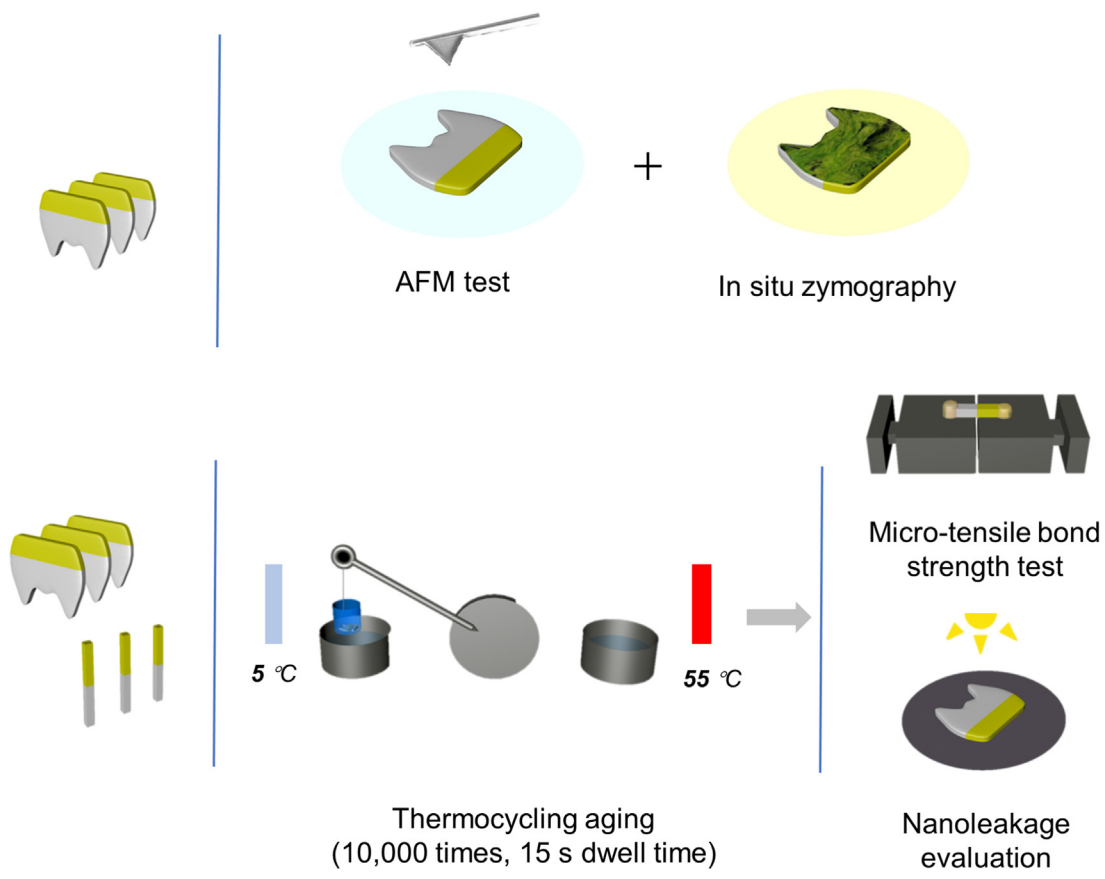
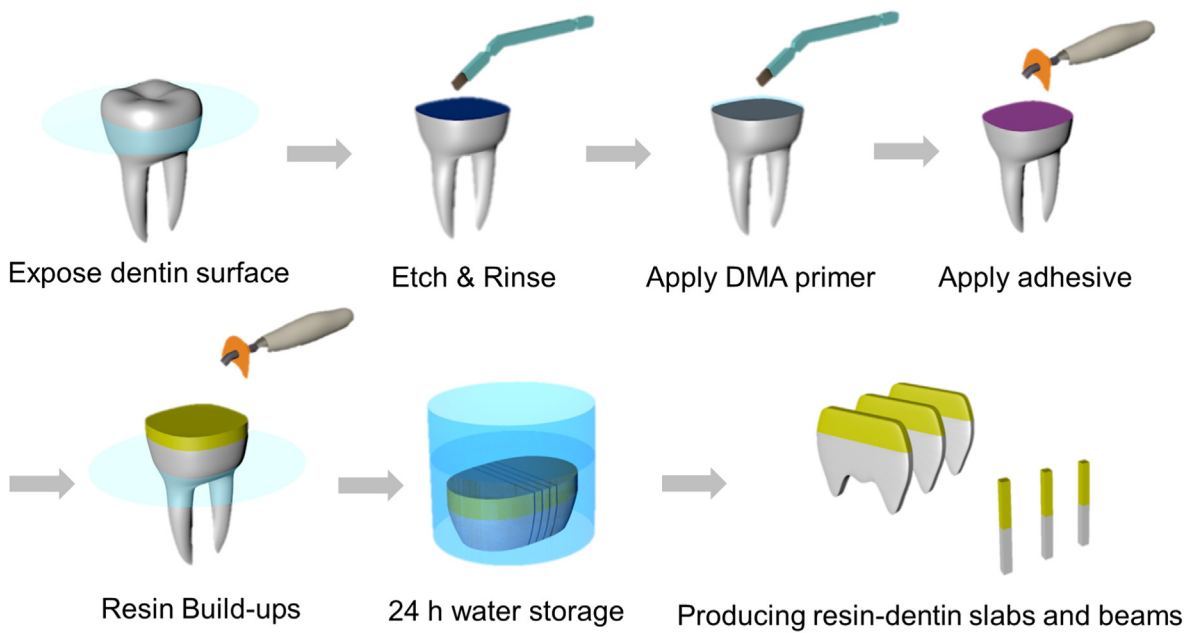


Fig. 2. The schematic procedures of dentin bonding and the related tests. The dentin surface was exposed, etched with phosphoric acid for 15 s, thoroughly rinsed with water spray, and applied with the DMA primer for 60 s. Adhesive was applied on the dentin surface followed by 20 s light-curing. Resin composite layers were built up on the dentin and polymerized with 20 s for each layer. After 24 h water storage, the bonded teeth were sectioned to produce resin-dentin slabs and beams for further test. Part of the slabs were subjected to AFM test and *in situ* zymography observation immediately, while the left slabs and beams were subjected to micro-tensile bond strength test and nanoleakage evaluation immediately or after 10,000 times thermocycling aging.

Table 1
Materials used, composition and application methods.

Material used	Manufacturer	Composition	Application methods
Scotchbond Universal Etchant	3 M ESPE, St. Paul, MN, USA	32% phosphoric acid; water	Apply etchant to dentin and react 15 s. Rinse thoroughly for 15 s with water spray.
Adper Single Bond 2	3 M ESPE, St. Paul, MN, USA	Bis-GMA; HEMA; dimethacrylates; initiators; water; and ethanol	Apply two coats of adhesive on the etched dentin surface for 15 s, and gently air thin for 5 s to evaporate solvents.
Filtek Z350 XT	3 M ESPE, St. Paul, MN, USA	Micro hybrid composite filled with barium glass particles	A layer (less than 1.5 mm) should be light cured for 20 s.

Abbreviations: Bis-GMA, bisphenol-A-diglycidylether dimethacrylate; HEMA, 2-hydroxyethyl methacrylate.

SEM at magnification of 400 \times under backscattered mode. The whole resin-dentin interface was scanned from the beginning to the end, and the percentage of silver particles deposition along the resin-dentin interface was calculated by Image J software (NIH, Frederick, MD, USA). The five slabs from each subgroup were tested in the same method and the average values of nanoleakage expression were analyzed by two-way ANOVA (Factors: DMA concentrations and aging) followed by *post hoc* Tukey's test ($\alpha = 0.05$) after validating the normality and homogeneity of the data.

2.9. *In situ* zymography of the resin-dentin interface

Four sound molars (one per DMA-EtOH group) were similarly prepared as Section 2.5 to produce 0.5 mm thick slabs with the resin-dentin interface exposed. The slabs were wet polished, ultrasonically cleaned, and placed on glass slides. The quenched fluorescein-conjugated gelatin reagent (E-12055, Molecular Probes, Eugene, OR, USA) was prepared according to the instruction before test, and 50 μ L solution was dropped on the top surface of each slab. The slabs were then covered by coverslips, and stored in humidified chamber for 24 h at 37 $^{\circ}$ C. The slabs were observed under confocal laser scanning microscopy (CLSM) (Olympus FV 1200, Tokyo, Japan) with an excitation/emission wavelength at 488 nm/530 nm. The green fluorescence detected within the resin-dentin interface indicates the activity of MMPs *in situ*.

2.10. Cytotoxicity test

Human dental pulp cells (HDPCs) were seeded at 5000 cells per well in 96-well plate and cultured in α -modified essential medium (HyClone, Logan, UT, USA) supplemented with 10% fetal bovine serum and 1% penicillin/streptomycin at 37 $^{\circ}$ C under conditions of 5% CO₂. DMA was dissolved in pure dimethyl sulfoxide (DMSO) with a series of

concentrations at 0, 1, 5, 10, 25, and 50 mmol/L, and filtrated to remove bacteria. Then DMA solution was diluted with culture medium at the ratio of 1:1000 into a series of concentrations at 0, 1, 5, 10, 25, and 50 μ mol/L. The vehicle control 0.1% DMSO was considered to be non-toxic for cells [35,36]. On 1, 3, and 5 days after incubation, the cells were collected for cell counting kit-8 (CCK-8) test. A 10 μ L volume of CCK-8 solution was added to each well, incubated for another 4 h, and the absorbance was measured under 450 nm with a microplate reader. The test was implemented in sextuplicate and the relative cell viability (%) with regard to the vehicle control within each incubation time was analyzed by one-way ANOVA followed by *post hoc* Tukey's test ($\alpha = 0.05$) after validating the normality and homogeneity of the data.

3. Results

3.1. Cross-linking between DMA with type I collagen

The representative TEM images of type I collagen treated by different DMA-EtOH solution was presented in Fig. 3. The type I collagen in the Control group (Fig. 3A) manifested a typical fibrillar network structure with many single fibrils connected with each other. While with the increase of DMA content (especially 10 mM DMA group, Fig. 3D), the

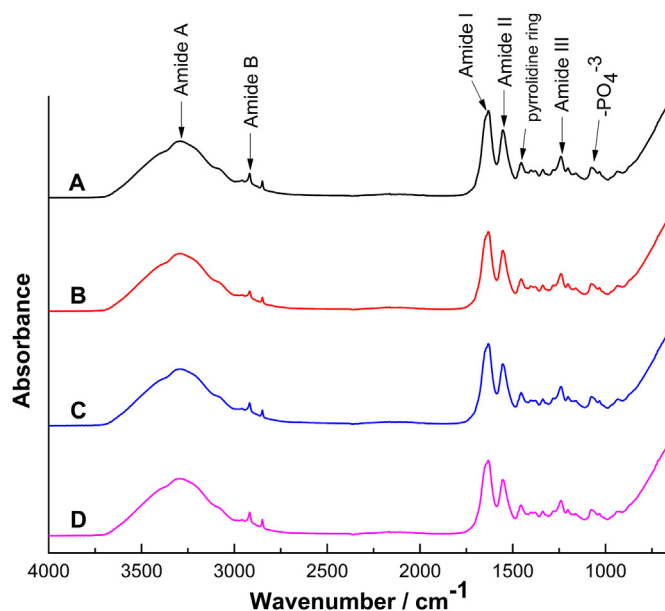


Fig. 4. Absorption spectrum in the infrared region of demineralized dentin matrix treated by different DMA contents for 60 min. The representative bands of collagen triple helix structure (Amide A, Amide B, Amide I, Amide II, and Amide III) existed after DMA treatment with no obvious change of the peak position. (A) Control, (B) 1 mM DMA, (C) 5 mM DMA, and (D) 10 mM DMA.

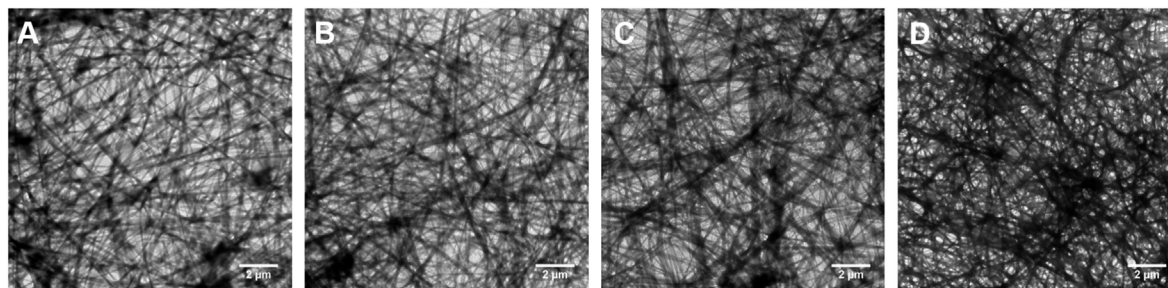


Fig. 3. Representative TEM images ($\times 2000$) of type I collagen treated by different groups. (A) Control, (B) 1 mM DMA, (C) 5 mM DMA, and (D) 10 mM DMA. With increasing concentration of DMA, the collagen fibrils were densely interconnected.

Table 2

The parameters of FTIR spectra of dentin matrix treated by different DMA solutions.

Treatment	Parameters		
	Amide I (cm^{-1})	Amide II (cm^{-1})	A_{1631}/A_{1450}
Control	1631.5	1552.8	1.21
1 mM DMA	1631.8	1552.8	1.22
5 mM DMA	1632.5	1552.4	1.20
10 mM DMA	1633.4	1552.4	1.20

Table 3

The influence of different concentrations of DMA on the degree of conversion of adhesive.

Treatment	Curing time	
	20s	120s
Control	20.93 (18.26–25.02) ^{Aa}	27.98 (25.09–28.81) ^{Ab}
1 mM DMA	19.91 (17.89–23.27) ^{Aa}	27.29 (25.87–27.96) ^{Ab}
5 mM DMA	19.26 (19.10–20.01) ^{Aa}	25.49 (23.85–26.31) ^{Ab}
10 mM DMA	19.68 (19.50–20.12) ^{Aa}	25.70 (24.69–26.54) ^{Ab}

Values of degree of conversion (%) are expressed as the median (25 percentile–75 percentile), $n = 6$. The groups identified by the same capital letter down the column are not statistically different ($p > 0.05$). The groups identified by the same lowercase letter across the row are not statistically different ($p > 0.05$).

collagen fibrils were densely tangled and overlapped with each other, with the number and size of interfibrillar spaces reduced apparently.

3.2. Influence of DMA on the structure of demineralized dentin matrix

The FTIR spectra of the interaction between DMA with demineralized dentin matrix was shown in Fig. 4. The representative parameters of FTIR spectra were presented in Table 2. It could be observed that all the representative bands of collagen triple helix structure existed after DMA treatment and there was no obvious change of the peak position except a minor shift of amide I band from 1631 to 1633 cm^{-1} .

3.3. Degree of conversion

The values of DC for the four groups after 20 s light curing and 100 s

post-polymerization were presented in Table 3. The results showed that there was no statistical difference among the four groups at both time points ($p > 0.05$). While after 100 s post-polymerization, the DC value had increased significantly in all groups compared with their 20 s value ($p < 0.05$).

3.4. DMT modulus of the resin-dentin interface

A representative SEM image of the resin-dentin interface was shown in Fig. 5A and the corresponding distribution of the DMT modulus was shown in Fig. 5B. Twenty ROIs were selected from the adhesive and hybrid layers from each specimen, respectively, and the statistical analysis result was shown in Table 4. There was no statistical difference in the DMT modulus of adhesive layer among the four groups ($p > 0.05$), while 10 mM DMA treatment had significantly increased the DMT modulus of the hybrid layer compared with that of Control group ($p < 0.05$).

3.5. Micro-tensile bond strength

Results of two-way ANOVA revealed that both the DMA concentrations ($F = 8.045$, $p < 0.001$) and aging ($F = 9.261$, $p = 0.003$) significantly affected the resin-dentin bond strength, while their interaction was not significant ($F = 2.302$, $p = 0.078$). The value of μTBS was presented in Table 5. No significant difference in the immediate μTBS was observed among the different groups ($p > 0.05$). However, after 10,000 times thermocycling aging, the μTBS of Control group dropped significantly compared with its immediate value ($p < 0.05$), while the μTBS of DMA-treated groups were well preserved with no significant difference compared with their immediate values ($p > 0.05$).

Table 4

The DMT modulus of specimens treated by different DMA solutions.

ROI	Control	1 mM DMA	5 mM DMA	10 mM DMA
Adhesive	7.25 ± 0.60^a	7.19 ± 0.58^a	7.09 ± 0.10^a	7.32 ± 0.08^a
Hybrid Layer	5.98 ± 0.41^a	6.14 ± 0.43^{ab}	6.26 ± 0.09^{ab}	6.95 ± 0.44^b

Values of DMT Modulus (GPa) of ROIs are expressed as the average \pm standard deviation, $n = 3$. Within each row, groups identified by the same lowercase letter are not statistically different ($p > 0.05$).

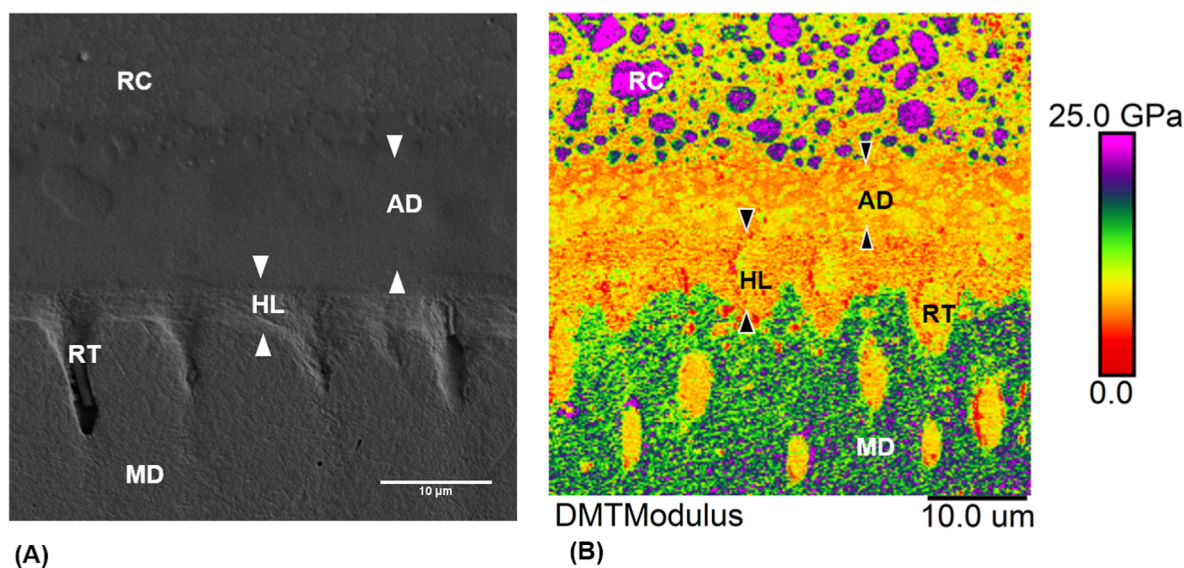


Fig. 5. The DMT modulus of the adhesive-dentin interface was analyzed by AFM. (A) SEM image of a representative adhesive-dentin interface. (B) Typical DMT modulus map obtained from PeakForce QNM scanning of the interface. The window of evaluation in (B) is not from the same location as shown in (A). Similar to SEM image, important features of the bonded interface were clearly presented in (B), including (RC) Resin Composite, (AD) Adhesive, (HL) Hybrid layer, (RT) Resin tag, and (MD) Mineralized dentin.

Table 5
Micro-tensile bond strength (μ TBS) of each group.

Groups	Treatment	
	24 h water storage	Thermocycling aging
Control	30.08 \pm 7.55 ^{Aa}	22.63 \pm 6.40 ^{Ab}
1 mM DMA	33.16 \pm 8.41 ^{Aa}	30.40 \pm 8.10 ^{Ba}
5 mM DMA	32.59 \pm 8.70 ^{Aa}	31.46 \pm 7.31 ^{Ba}
10 mM DMA	32.73 \pm 7.39 ^{Aa}	31.85 \pm 8.10 ^{Ba}

The μ TBS value (MPa) (n = 30) of each group are expressed as means \pm standard deviation. The groups identified by the same capital letter down the column are not statistically different ($p > 0.05$). The groups identified by the same lowercase letter across the row are not statistically different ($p > 0.05$).

3.6. Failure mode analysis

The percentage distribution of the failure mode and the results of Chi-Square test were shown in Fig. 6. Among the immediate values, even though there was no significant difference among the different groups, the p -value was very close to 0.05 ($p = 0.064$), indicating that DMA treatment had strengthened the integrity of the resin-dentin interface to some extent. By contrast, the percentage of CD mode increased dramatically in the Control group after aging, while significantly fewer M2 and CD failures were observed in DMA-treated groups ($p < 0.05$). The representative SEMs of different failure modes were shown in Fig. 7.

3.7. Nanoleakage evaluation

Results of two-way ANOVA revealed that the DMA concentrations ($F = 14.636$, $p < 0.001$) significantly affected the deposition of nanoleakage, while aging ($F = 0.140$, $p = 0.711$) and their interaction was not significant ($F = 2.601$, $p = 0.075$). The value of nanoleakage expression was presented in Table 6. The aged value of Control group had increased significantly compared with other groups ($p < 0.05$), which indicated that the integrity of resin-dentin interface was well protected by DMA treatment after thermocycling aging. The representative SEM images of nanoleakage expression were presented in Fig. 8. After aging, a thick, continuous deposition of silver particles could be observed along the resin-dentin interface, and sometimes even filled the dentinal tubules of Control group (Fig. 8a). On the contrary, there was only an interrupted, sparse distribution of silver particles in DMA-treated groups (Fig. 8b, c, & d).

3.8. In situ zymography of the resin-dentin interface

The representative CLSM images of *in situ* zymography from the different groups were presented in Fig. 9. An intense green fluorescence could be observed not only in the interface of the Control group (Fig. 9A), but also occupied nearly every corner of the dentinal tubules, indicating the strong activity of endogenous MMPs at these sites. With the increase of DMA concentration, the intensity of green fluorescence had dramatically decreased in the specimens, not only limited inside the resin-dentin interface, but also around 50 μ m dentin matrix beneath the interface which could be infiltrated by DMA.

3.9. Cytotoxicity test

The result of cytotoxicity evaluation was presented in Fig. 10. After 1-day incubation, all the DMA-treated groups presented an acceptable cell viability compared with the vehicle control ($p > 0.05$). However, after 5-day incubation, only the highest concentration of DMA group (50 μ mol/L) manifested a significant reduction (47.96% cell viability) compared with the vehicle control ($p < 0.05$), while the relative cell viability of other DMA concentrations was still over 80% with no significant difference compared with the vehicle control ($p > 0.05$).

4. Discussion

The resin monomers can be basically classified as cross-linker monomers and functional monomers [37]. The cross-linker monomers have two or more polymerizable groups (vinyl group or carbon-carbon double bond) and serve as the backbone to provide the mechanical strength of adhesive. The functional monomers are distinguished by their unique functional groups, which will impart monomer specific function to modify the performance of adhesive [38]. In the current study, in order to retain the wet bonding property of MAP and its ability to polymerize with adhesive monomers, DMA was selected and evaluated as a potential mussel-inspired functional monomer in dentin bonding. The results showed that DMA could successfully (1) cross-link with dentin collagen via non-covalent bonds, (2) polymerize with adhesive without affecting the degree of conversion and elastic modulus, (3) strengthen the integrity of resin-dentin interface and prolong the durability of resin-dentin bond, and (4) inhibit the activity of endogenous MMPs. Therefore, except the second null hypothesis that could not be rejected, all the remaining null

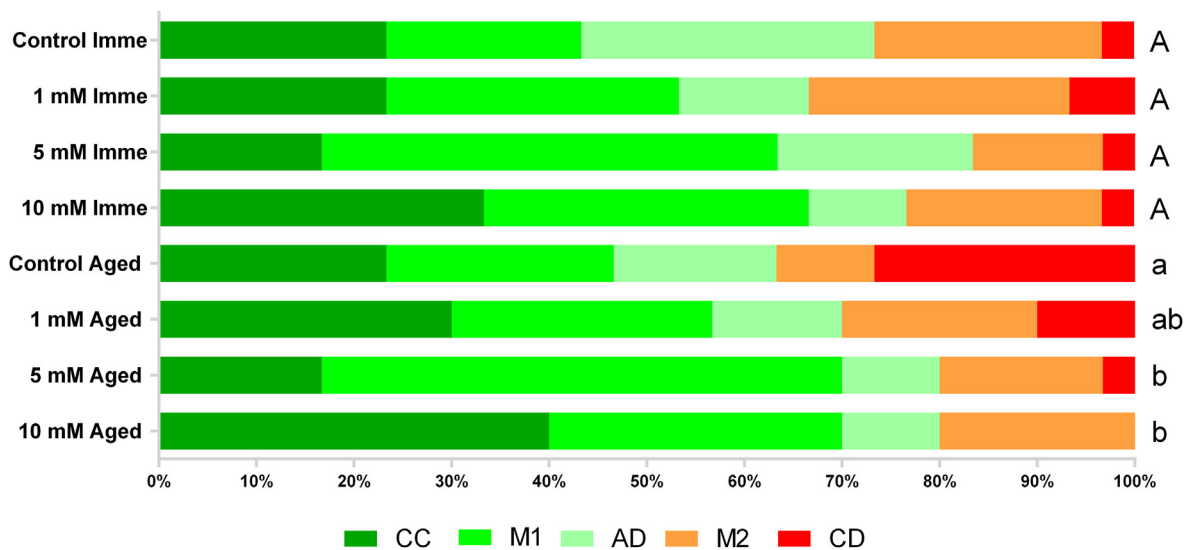


Fig. 6. Distribution of failure patterns (%) after micro-tensile bond strength test. (CC) Cohesive failure in composite. (AD) Adhesive failure. (CD) Cohesive failure in dentin. (M1) Mixed failure of AD + CC. (M2) Mixed failure of AD + CD. Groups identified by the same capital letter indicated no significant differences among the immediate values ($p > 0.05$). Groups identified by the same lowercase letter indicated no significant differences among the aged values ($p > 0.05$).

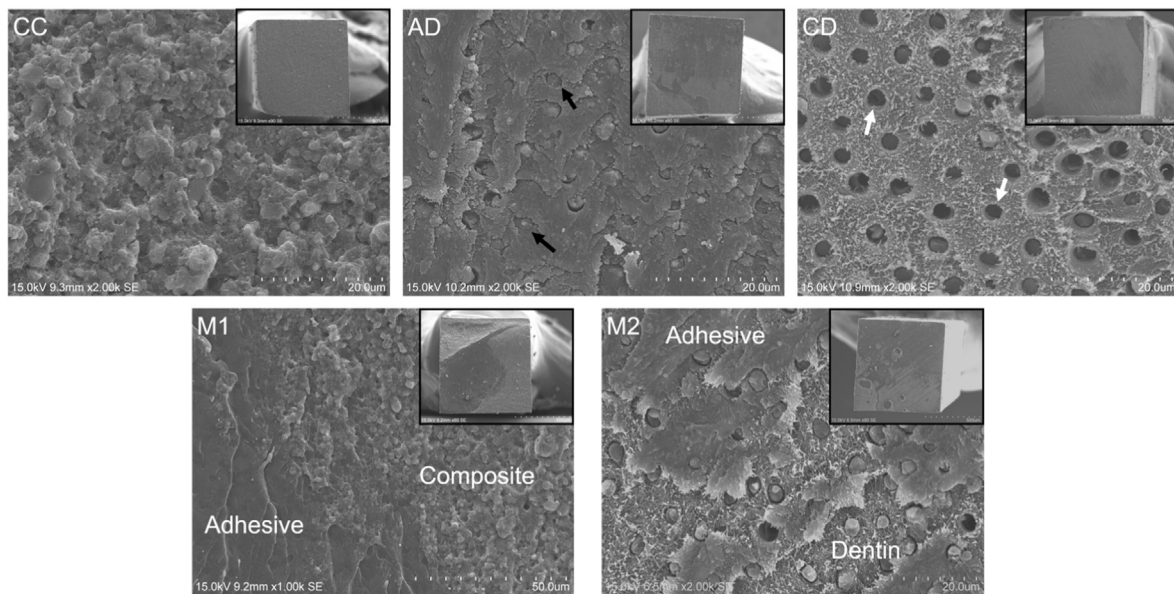


Fig. 7. Representative SEM images of the failure modes (2000 X). The overall conditions of the fractured beams were illustrated at the upper right corner (90 X). (CC) Cohesive failure in composite. Failure occurred at the composite layer with no resin tags observed. (AD) Adhesive failure. The resin tags (indicated by black arrows) appeared under the adhesive layer with no collagen matrix exposed. (CD) Cohesive failure in dentin. Failure occurred at the bottom part of the hybrid layer with collagen matrix and dentinal tubules (indicated by white arrows) exposed. (M1) Mixed failure of CC + AD. (M2) Mixed failure of AD + CD.

Table 6
The percentage of nanoleakage deposition (%) of each group.

Groups	Treatment	
	24 h water storage	Thermocycling aging
Control	36.57 ± 3.79 ^{Aa}	50.41 ± 4.82 ^{Ab}
1 mM DMA	38.45 ± 11.79 ^{Aa}	34.76 ± 12.31 ^{Ba}
5 mM DMA	20.92 ± 7.87 ^{Aa}	20.92 ± 3.36 ^{Ba}
10 mM DMA	27.31 ± 8.21 ^{Aa}	21.29 ± 4.13 ^{Ba}

The percentage of nanoleakage deposition (%) (n = 5) of each group are expressed as means ± standard deviation. The groups identified by the same capital letter down the column are not statistically different (p > 0.05). The groups identified by the same lowercase letter across the row are not statistically different (p > 0.05).

hypotheses should be rejected.

As illustrated in Fig. 3, the TEM images directly reveal the cross-linking effect of DMA on collagen structure at the microscale level. The

rationale behind the DMA-collagen interaction was further explored by ATR-FTIR. The special triple helix conformation of type I collagen is characterized by its featured amide bands [39]. The amide A band (3300 cm⁻¹) and amide B band (2917 cm⁻¹) represent the stretching vibrations of N-H and O-H groups. In the fingerprint region of collagen, the amide I band at 1630 cm⁻¹ (mainly C=O stretching) and amide II band at 1552 cm⁻¹ (C-N stretching coupled with N-H bending) are sensitive to the change in the secondary structure of proteins [40]. The amide III band at 1240 cm⁻¹ is mainly attributed to the C-N stretching and N-H deformation. The peak identified in 1450 cm⁻¹ represents the pyrrolidine rings of proline and hydroxyproline, which serves as a useful internal standard and the absorption ratios of Amide III to pyrrolidine ring (A_{III}/A₁₄₅₀) could be used as a parameter to judge the integrity of collagen triple helices [41,42]. From Fig. 4, we could observe that all the representative bands of collagen triple helix structure existed and there was no obvious appearance of new bands after DMA treatment, which indicated the interaction between DMA with collagen was attributed to the formation of non-covalent bonds [40]. From Table 2, there was a

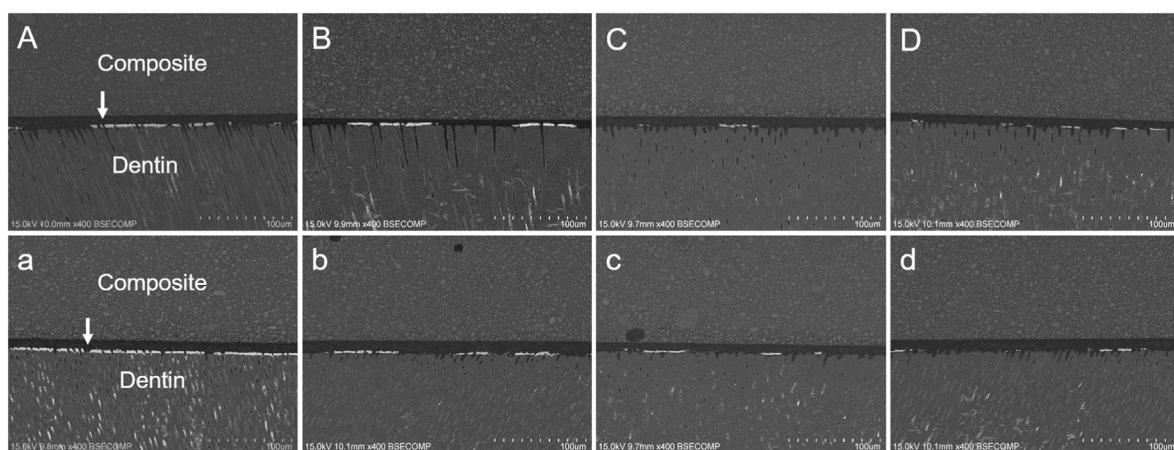


Fig. 8. Representative SEM images of nanoleakage expression from different groups (400 X). (A–D) The immediate groups. (a–d) The 10,000 times thermocycling aged groups. (A,a) Control; (B,b) 1 mM DMA; (C,c) 5 mM DMA; and (D,d) 10 mM DMA. The white arrows indicated the deposition of silver particle along the adhesive-dentin interface.

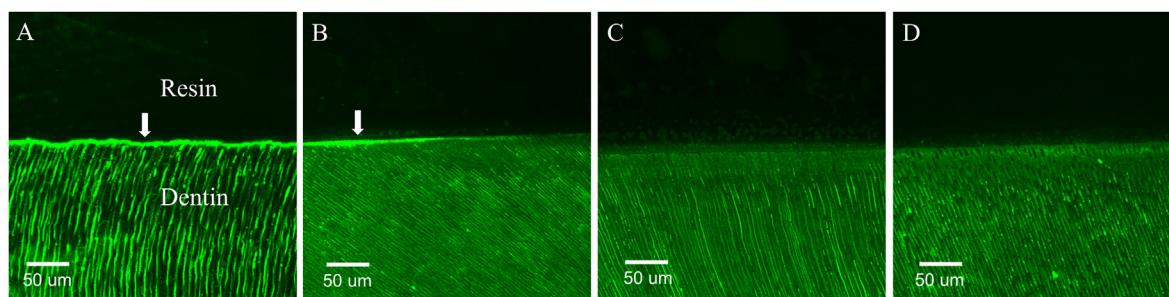


Fig. 9. Confocal laser scanning microscopy images of *in situ* zymography labeled with quenched fluorescein-conjugated gelatin. (A) Control; (B) 1 mM DMA; (C) 5 mM DMA; and (D) 10 mM DMA. The green fluorescence detected within the resin-dentin interface (indicated by white arrows) represented the activity of MMPs *in situ*.

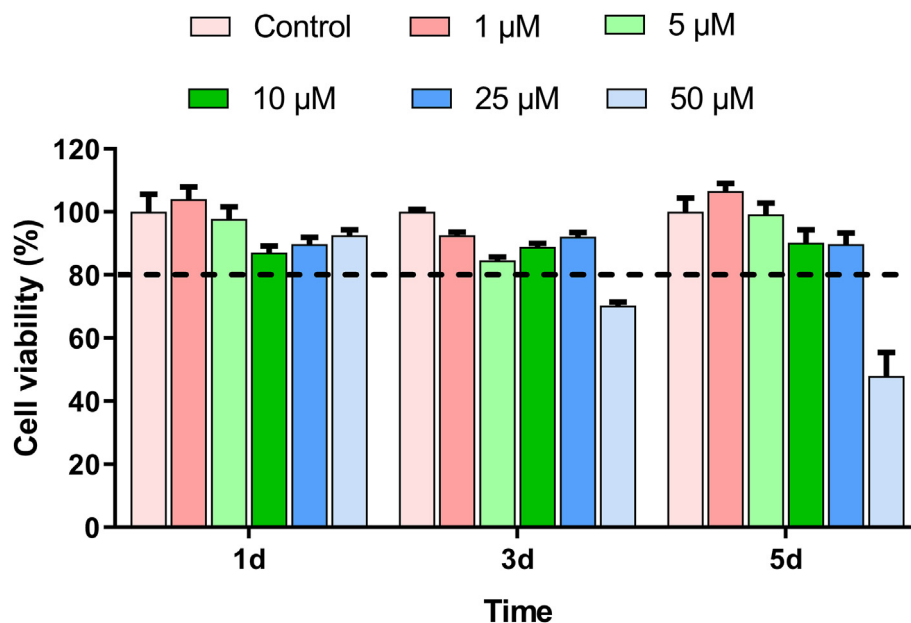


Fig. 10. Relative cell viability of HDPCs exposed to different concentrations of DMA primer at 1, 3, and 5 days.

small shift of the amide I band from 1631 to 1633 cm^{-1} , which indicated the potential hydrogen bond between DMA with collagen matrix [43]. As for the ratio of A_{III}/A_{1450} , the values for all groups were higher than 1.00 with no major difference, which indicated the ordered collagen structure of dentin matrix was not destructed by DMA, since the ratio for the denatured collagen is around 0.6 [41,44].

After validating the cross-linking function of the catechol group, the polymerizable property of the carbon-carbon double bond of DMA was evaluated by examining the degree of adhesive conversion. The polymerization reaction can be roughly divided into two steps: (1) the light irradiation of the initiators to start the reaction and release free radicals within the first 10–20 s, and (2) the autonomous reaction between free radicals with neighboring resin monomers to continue the chain growth polymerization for hours [45]. Therefore, two time set points (20 s light curing and 100 s post-polymerization reaction) were selected in the current study. The results from Table 3 showed that the addition of DMA had no influence on the initial light irradiation and the following free radical chain reaction of adhesive, which indicated the successful co-polymerization of DMA with adhesive monomers.

The influence of DMA on the elastic modulus of adhesive and hybrid layers was further estimated by AFM using PeakForce QNM mode. Comparing with the traditional quasi-static nanoindentation test, the PeakForce QNM mode could provide a much higher resolution of the scanning area and produce the mapping image simultaneously [46]. As

illustrated in Fig. 5, similar to the representative SEM images, important features of the bonded interface could clearly be distinguished in the AFM tapping image, which facilitated us to calculate the DMT modulus of adhesive and hybrid layers separately and accurately. On one side, no difference was detected within the adhesive layer among all groups, which supported the conclusion that DMA could polymerize with resin monomers without hampering the mechanical strength of adhesive. On the other side, the DMT modulus of the hybrid layer increased with higher DMA concentration. This result was in accordance with the TEM observation, that the formation of hydrogen bond between DMA with dentin collagen had greatly strengthened the integrity of the hybrid layer. The higher elastic modulus of DMA-treated hybrid layer enabled it to absorb more energy under the external force and thus had a higher probability of preventing resin-dentin bond failure caused by sudden stress change.

Based on the above results, we could draw the preliminary conclusion that DMA has the capability to act as a functional monomer in dental adhesive. The possible rationale is illustrated in Fig. 11. From a visual perspective, DMA could be deemed as a “bridge” connecting the upper adhesive network via carbon-carbon double bond polymerization and lower dentin collagen fibrils via hydrogen bond, unifying them as one whole structure to resist various external attacks from the harsh oral environment. For the “bridge” itself, the hydrolysis resistance of amide bond is much stronger than that of ester bond [29], which provides a

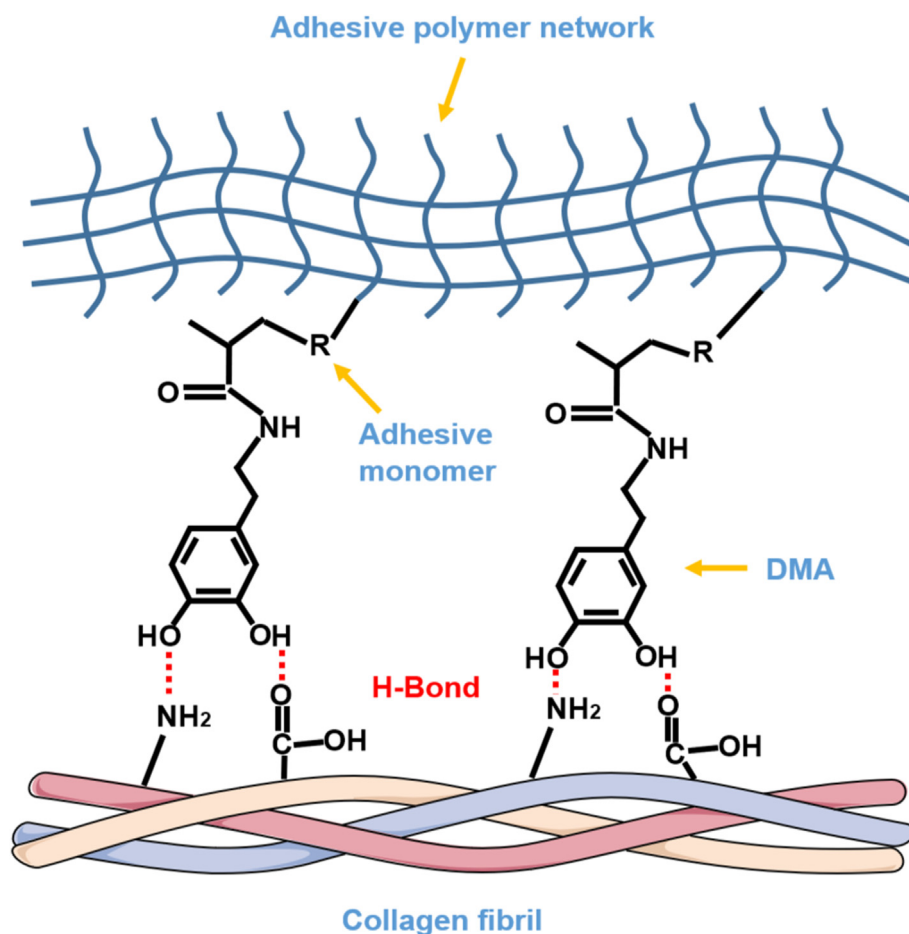


Fig. 11. The possible rationale of DMA as a functional monomer in dentin bonding. DMA could be deemed as a “bridge” connecting the upper adhesive network via carbon-carbon double bond polymerization and lower dentin collagen fibrils via hydrogen bond, unifying them as one whole structure.

theoretical basis for the durable wet adhesion property of DMA. Bearing this image in mind, the dentin bonding performance of DMA-EtOH primer was comprehensively evaluated.

The thermocycling aging process (10,000 times, 5–55 °C, 15 s dwell time and 7 s transferring time) is used to assess bond durability by simulating the daily changes of intraoral temperature on eating, drinking and breathing habits [47]. Due to the discrepancy between the coefficients of expansion and contraction between resin and dentin, the repeated thermocycling aging can create volumetric changes within the resin-dentin interface, leading to the formation of cracks and fissures over time [47]. However, as mentioned previously, DMA could bridge the adhesive and dentin collagen as a whole structure. This property has rendered the DMA-treated interface a much higher strength to resist the thermal strains aggregated, and decrease cracks formation consequently. Therefore, the μ TBS values for the Control group decreased significantly after aging, while DMA-treated groups had no obvious change. Meanwhile, the percentage of failure occurred at the bottom part of the hybrid layer was significantly higher in the Control group than the DMA-treated groups.

In addition to μ TBS, nanoleakage is also an effective indicator for evaluating the sealing capability and quality of the resin-dentin interface [48,49]. Due to the formation of cracks and fissures after thermocycling aging, these voids enabled the infiltration and deposition of silver particles along the bonded interface. Therefore, the amount of silver deposition clearly reflected the water-filled and degraded areas along the interface. From Table 6 and Fig. 8, we could observe that only the Control group had a significant increase of nanoleakage expression after aging, while DMA-treated groups had no significant change. Meanwhile, the

immediate nanoleakage values of 5 and 10 mM DMA groups were relatively lower than 1 mM DMA and Control groups, which indicated that 5 and 10 mM DMA-EtOH primer could reduce the amount of remnant water within the hybrid layer immediately, and that would be beneficial for the resin-dentin bond durability [4]. Apart from the aforementioned “bridge” function of DMA, one more possible mechanism might explain this phenomenon. The collagen network is a porous structure that provides space and voids for the infiltration of free water and silver ions. However, the cross-linking effect of DMA obviously reduced the porosity of collagen network, thereby decrease the nanoleakage distribution accordingly [50].

The degradation of dentin collagen is not only attributed to water hydrolysis, the endogenous MMPs also play an important role in the degradation of collagen fibrils and the destruction of the resin-dentin interface [51]. Targeting at the catalytic Zn²⁺ and Ca²⁺ ions of MMPs, various MMP inhibitors have been synthesized and applied in clinical treatment [27]. Considering the strong chelation ability of the catechol group with metal ions, Rubino et al. [28] evaluated the inhibitory performance of the catechol group against various MMPs, including MMP-2 (IC₅₀ = 0.59 μ M), MMP-8 (IC₅₀ = 10.0 μ M), MMP-9 (IC₅₀ = 57.0 μ M) and MMP-14 (IC₅₀ = 6.2 μ M). The results demonstrated the broad-spectrum inhibitory effects of catechol group. Tauro et al. [52] also reported that the catechol group may induce the conformational changes of the 3D structure of MMPs by intruding into the specific S₁' pocket, thus imposing selective inhibition effect. Apart from the anti-proteolytic ability, the cross-linking effect of DMA may also strengthen the mechanical integrity of collagen fibrils, and reduce the potential cleavage sites of MMPs simultaneously. Therefore, in the current *in situ*

zymography observation, the intensity of green fluorescence emitted in the DMA-treated groups was significantly decreased compared with the Control group.

Cytotoxicity evaluation is definitely indispensable when applying novel synthesized materials in human body. Right now, several published articles have reported the biocompatibility of mussel-inspired compounds in clinical application, including medical sealants [53,54], imaging agents [55,56], antifouling coatings [57,58] and adhesives [59, 60], etc. In the current *in vitro* evaluation, a significant cytotoxicity of DMA was observed in the 50 μM concentration (47.96% cell viability) after 5-day incubation (Fig. 10), while the cell viability was all over 80% for the lower concentrations of DMA. Therefore, the LC₅₀ value of DMA was between 25 μM and 50 μM (equaled to 5.5–11 $\mu\text{g}/\text{mL}$) based on the current results, which was similar to the widely used resin monomer bisphenol A glycerolate dimethacrylate (Bis-GMA) (LC₅₀ value was between 5–10 $\mu\text{g}/\text{mL}$) [61]. Besides, due to the continuous outward pressure generated by dentinal fluid, it would be difficult for such small amount of DMA primer (only one or two drops in clinical application) to penetrate through the long dentinal tubules [48]. Therefore, in consistent with previously published results confirming the high biocompatibility of mussel-inspired compounds, DMA could also be used as a potential biocompatible functional monomer in dentin bonding *in vivo*.

Despite the relatively acceptable performance of DMA as a potential functional monomer in dentin bonding, the easily oxidized property of the catechol group has limited the shelf-life of DMA primer. In the current research, the color of DMA-EtOH solution would turn into faint yellow after two months usage, and that would be unpractical to be transferred into clinical practice. Therefore, future studies may consider incorporate a proper amount of commercial antioxidants inside DMA primer without affecting the polymerization of dental adhesive [62].

5. Conclusion

DMA could be used as a functional monomer in dentin bonding system with high biocompatibility. One-minute pretreatment of DMA-EtOH primer could strengthen the integrity of resin-dentin interface, inhibit the activities of endogenous MMPs, and prolong resin-dentin bond durability effectively.

CRediT author statement

Kang Li: Conceptualization, Methodology, Investigation, Formal analysis, Resources, Writing-Original Draft. **Chenmin Yao:** Methodology, Investigation, Validation, Writing - Review & Editing. **Yuhong Sun:** Methodology, Investigation, Resources. **Kun Wang:** Methodology, Investigation. **Xiangtao Wang:** Methodology, Investigation. **Zhengzhi Wang:** Methodology, Investigation. **James Kit Hon Tsoi:** Supervision, Writing - Review & Editing. **Cui Huang:** Supervision, Writing - Review & Editing, Funding acquisition. **Cynthia Kar Yung Yiu:** Supervision, Writing - Review & Editing, Funding acquisition.

Declaration of competing interest

The authors declare that they have no known competing financial interests or personal relationships that could have appeared to influence the work reported in this paper.

Acknowledgements

This work was financially supported by HKU seed fund for basic research (grant no. 201811159154, 201910159147) and National Nature Science Foundation of China (grant no. 81771112).

References

- [1] V. Moraschini, C.K. Fai, R.M. Alto, G.O.D. Santos, Amalgam and resin composite longevity of posterior restorations: a systematic review and meta-analysis, *J. Dent.* 43 (2015) 1043–1050, <https://doi.org/10.1016/j.jdent.2015.06.005>.
- [2] J.M. Broadbent, C.M. Murray, D.R. Schwass, M. Brosnan, P.A. Brunton, K.S. Lyons, W.M. Thomson, The dental amalgam phasedown in New Zealand: a 20-year trend, *Operat. Dent.* 45 (2020) 255–264, <https://doi.org/10.2341/19-024-c>.
- [3] L. Tjäderhane, Dentin bonding: can we make it last? *Operat. Dent.* 40 (2015) 4–18, <https://doi.org/10.2341/14-095-bl>.
- [4] D.H. Pashley, F.R. Tay, R.M. Carvalho, F.A. Rueggeberg, K.A. Agee, M. Carrilho, A. Donnelly, F. Garcia-Godoy, From dry bonding to water-wet bonding to ethanol-wet bonding. A review of the interactions between dentin matrix and solvated resins using a macromodel of the hybrid layer, *Am. J. Dent.* 20 (2007) 7–20.
- [5] P. Spencer, Y. Wang, Adhesive phase separation at the dentin interface under wet bonding conditions, *J. Biomed. Mater. Res.* 62 (2002) 447–456, <https://doi.org/10.1002/jbm.10364>.
- [6] D.H. Pashley, F.R. Tay, L. Breschi, L. Tjäderhane, R.M. Carvalho, M. Carrilho, A. Tezvergil-Mutluay, State of the art etch-and-rinse adhesives, *Dent. Mater.* 27 (2011) 1–16, <https://doi.org/10.1016/j.dental.2010.10.016>.
- [7] L. Breschi, T. Maravic, S.R. Cunha, A. Comba, M. Cadenaro, L. Tjäderhane, D.H. Pashley, F.R. Tay, A. Mazzoni, Dentin bonding systems: from dentin collagen structure to bond preservation and clinical applications, *Dent. Mater.* 34 (2018) 78–96, <https://doi.org/10.1016/j.dental.2017.11.005>.
- [8] C.P. Gré, D.P. Lise, A.P. Ayres, J. De Munck, A. Tezvergil-Mutluay, R. Seseogullari-Dirihan, G.C. Lopes, K. Van Landuyt, B. Van Meerbeek, Do collagen cross-linkers improve dentin's bonding receptiveness? *Dent. Mater.* 34 (2018) 1679–1689, <https://doi.org/10.1016/j.dental.2018.08.303>.
- [9] E.L. Kostoryz, K. Dharmala, Q. Ye, Y. Wang, J. Huber, J.G. Park, G. Snider, J.L. Katz, P. Spencer, Enzymatic biodegradation of HEMA/bisGMA adhesives formulated with different water content, *J. Biomed. Mater. Res. B Appl. Biomater.* 88 (2009) 394–401, <https://doi.org/10.1002/jbm.b.31095>.
- [10] M.H. Ahmed, K. Yoshihara, C. Yao, Y. Okazaki, K. Van Landuyt, M. Peumans, B. Van Meerbeek, Multiparameter evaluation of acrylamide HEMA alternative monomers in 2-step adhesives, *Dent. Mater.* 37 (2021) 30–47, <https://doi.org/10.1016/j.dental.2020.10.002>.
- [11] D. Eltahlah, C.D. Lynch, B.L. Chadwick, I.R. Blum, N.H.F. Wilson, An update on the reasons for placement and replacement of direct restorations, *J. Dent.* 72 (2018) 1–7, <https://doi.org/10.1016/j.jdent.2018.03.001>.
- [12] E.D. Roumanas, The frequency of replacement of dental restorations may vary based on a number of variables, including type of material, size of the restoration, and caries risk of the patient, *J. Evid. Base Dent. Pract.* 10 (2010) 23–24, <https://doi.org/10.1016/j.jebdp.2009.11.009>.
- [13] M.K. Ayar, A review of ethanol wet-bonding: principles and techniques, *Eur. J. Dermatol.* 10 (2016) 155–159, <https://doi.org/10.4103/1305-7456.175687>.
- [14] L. Niu, W. Zhang, D.H. Pashley, L. Breschi, J. Mao, J. Chen, F.R. Tay, Biomimetic remineralization of dentin, *Dent. Mater.* 30 (2014) 77–96, <https://doi.org/10.1016/j.dental.2013.07.013>.
- [15] E. Kuhn, P. Farhat, A.P. Teitelbaum, A. Mena-Serrano, A.D. Loguercio, A. Reis, D.H. Pashley, Ethanol-wet bonding technique: clinical versus laboratory findings, *Dent. Mater.* 31 (2015) 1030–1037, <https://doi.org/10.1016/j.dental.2015.05.010>.
- [16] C.Y. Cao, M.L. Mei, Q.L. Li, E.C.M. Lo, C.H. Chu, Methods for biomimetic remineralization of human dentine: a systematic review, *Int. J. Mol. Sci.* 16 (2015) 4615–4627, <https://doi.org/10.3390/ijms16034615>.
- [17] B.P. Lee, P.B. Messersmith, J.N. Israelachvili, J.H. Waite, Mussel-inspired adhesives and coatings, *Annu. Rev. Mater. Res.* 41 (2011) 99–132, <https://doi.org/10.1146/annurev-matsci-062910-100429>.
- [18] N. Pandey, L.F. Soto-Garcia, J. Liao, P. Zimmern, K.T. Nguyen, Y. Hong, Mussel-inspired bioadhesives in healthcare: design parameters, current trends, and future perspectives, *Biomater. Sci.* 8 (2020) 1240–1255, <https://doi.org/10.1039/c9bm01848d>.
- [19] J.H. Ryu, P.B. Messersmith, H. Lee, Polydopamine surface chemistry: a decade of discovery, *ACS Appl. Mater. Interfaces* 10 (2018) 7523–7540, <https://doi.org/10.1021/acsami.7b19865>.
- [20] J.H. Waite, N.H. Andersen, S. Jewhurst, C. Sun, Mussel adhesion: finding the tricks worth mimicking, *J. Adhes.* 81 (2005) 297–317, <https://doi.org/10.1080/00218460590944602>.
- [21] H. Li, M.F. Burrow, M.J. Tyas, The effect of load cycling on the nanoleakage of dentin bonding systems, *Dent. Mater.* 18 (2002) 111–119, [https://doi.org/10.1016/s0109-5641\(01\)00029-x](https://doi.org/10.1016/s0109-5641(01)00029-x).
- [22] C. Loke, J. Lee, S. Sander, L. Mei, M. Farella, Factors affecting intra-oral pH—a review, *J. Oral Rehabil.* 43 (2016) 778–785, <https://doi.org/10.1111/joor.12429>.
- [23] S. Zhang, M. Kern, The role of host-derived dentinal matrix metalloproteinases in reducing dentin bonding of resin adhesives, *Int. J. Oral Sci.* 1 (2009) 163–176, <https://doi.org/10.4248/ijos.09044>.
- [24] S.B. Lee, C. González-Cabezas, K.M. Kim, K.N. Kim, K. Kuroda, Catechol-functionalized synthetic polymer as a dental adhesive to contaminated dentin surface for a composite restoration, *Biomacromolecules* 16 (2015) 2265–2275, <https://doi.org/10.1021/acs.biomac.5b00451>.
- [25] H. Fang, Q.L. Li, M. Han, M.L. Mei, C.H. Chu, Anti-proteolytic property and bonding durability of mussel adhesive protein-modified dentin adhesive interface, *Dent. Mater.* 33 (2017) 1075–1083, <https://doi.org/10.1016/j.dental.2017.07.008>.

- [26] N.R.M. Rodriguez, S. Das, Y. Kaufman, W. Wei, J.N. Israelachvili, J.H. Waite, Mussel adhesive protein provides cohesive matrix for collagen type-1 α , *Biomaterials* 51 (2015) 51–57, <https://doi.org/10.1016/j.biomaterials.2015.01.033>.
- [27] K. Li, F.R. Tay, C.K.Y. Yiu, The past, present and future perspectives of matrix metalloproteinase inhibitors, *Pharmacol. Ther.* 207 (2020) 107465, <https://doi.org/10.1016/j.pharmthera.2019.107465>.
- [28] M.T. Rubino, D. Maggi, A. Laghezza, F. Loiodice, P. Tortorella, Identification of novel matrix metalloproteinase inhibitors by screening of phenol fragments library, *Arch. Pharm.* 344 (2011) 557–563, <https://doi.org/10.1002/ardp.201000350>.
- [29] S.B. Rodrigues, F.M. Collares, V.C. Leitune, L.F. Schneider, F.A. Oglari, C.L. Petzhold, S.M. Samuel, Influence of hydroxyethyl acrylamide addition to dental adhesive resin, *Dent. Mater.* 31 (2015) 1579–1586, <https://doi.org/10.1016/j.dental.2015.10.005>.
- [30] D.J. Epasinghe, M.F. Burrow, C.K.Y. Yiu, Effect of proanthocyanidin on ultrastructure and mineralization of dentine collagen, *Arch. Oral Biol.* 84 (2017) 29–36, <https://doi.org/10.1016/j.archoralbio.2017.09.012>.
- [31] Z. Wang, K. Wang, W. Xu, X. Gong, F. Zhang, Mapping the mechanical gradient of human dentin-enamel-junction at different intratooth locations, *Dent. Mater.* 34 (2018) 376–388, <https://doi.org/10.1016/j.dental.2017.11.001>.
- [32] H. Ryou, L.N. Niu, L. Dai, C.R. Pucci, D.D. Arola, D.H. Pashley, F.R. Tay, Effect of biomimetic remineralization on the dynamic nanomechanical properties of dentin hybrid layers, *J. Dent. Res.* 90 (2011) 1122–1128, <https://doi.org/10.1177/0022034511414059>.
- [33] K. Li, Y. Sun, J.K.H. Tsoi, C.K.Y. Yiu, The application of mussel-inspired molecule in dentin bonding, *J. Dent.* 99 (2020) 103404, <https://doi.org/10.1016/j.jdent.2020.103404>.
- [34] F.R. Tay, D.H. Pashley, M. Yoshiyama, Two modes of nanoleakage expression in single-step adhesives, *J. Dent. Res.* 81 (2002) 472–476, <https://doi.org/10.1177/154405910208100708>.
- [35] P.A. Tsuji, T. Walle, Cytotoxic effects of the dietary flavones chrysin and apigenin in a normal trout liver cell line, *Chem. Biol. Interact.* 171 (2008) 37–44, <https://doi.org/10.1016/j.cbi.2007.08.007>.
- [36] W. Qi, D. Ding, R.J. Salvi, Cytotoxic effects of dimethyl sulphoxide (DMSO) on cochlear organotypic cultures, *Hear. Res.* 236 (2008) 52–60, <https://doi.org/10.1016/j.heares.2007.12.002>.
- [37] G. Vasudeva, Monomer systems for dental composites and their future: a review, *J. Calif. Dent. Assoc.* 37 (2009) 389–398.
- [38] K.L. Van Landuyt, J. Snauwaert, J. De Munck, M. Peumans, Y. Yoshida, A. Poitevin, E. Coutinho, K. Suzuki, P. Lambrechts, B. Van Meerbeek, Systematic review of the chemical composition of contemporary dental adhesives, *Biomaterials* 28 (2007) 3757–3785, <https://doi.org/10.1016/j.biomaterials.2007.04.044>.
- [39] B.B. Doyle, E.G. Bendit, E.R. Blout, Infrared spectroscopy of collagen and collagen-like polypeptides, *Biopolymers* 14 (1975) 937–957, <https://doi.org/10.1002/bip.1975.360140505>.
- [40] X. Yang, D. Wu, Z. Du, R. Li, X. Chen, X. Li, Spectroscopy study on the interaction of quercetin with collagen, *J. Agric. Food Chem.* 57 (2009) 3431–3435, <https://doi.org/10.1021/jf803671s>.
- [41] L. He, C. Mu, J. Shi, Q. Zhang, B. Shi, W. Lin, Modification of collagen with a natural cross-linker, procyanidin, *Int. J. Biol. Macromol.* 48 (2011) 354–359, <https://doi.org/10.1016/j.ijbiomac.2010.12.012>.
- [42] S.B. Botta, P.A. Ana, M.O. Santos, D.M. Zzell, A.B. Matos, Effect of dental tissue conditioners and matrix metalloproteinase inhibitors on type I collagen microstructure analyzed by Fourier transform infrared spectroscopy, *J. Biomed. Mater. Res. B Appl. Biomater.* 100 (2012) 1009–1016, <https://doi.org/10.1002/jbm.b.32666>.
- [43] C.S. Ku, M. Sathishkumar, S.P. Mun, Binding affinity of proanthocyanidin from waste *Pinus radiata* bark onto proline-rich bovine achilles tendon collagen type I, *Chemosphere* 67 (2007) 1618–1627, <https://doi.org/10.1016/j.chemosphere.2006.11.037>.
- [44] G. Goissis, L. Piccirilli, J.C. Goes, A.M. de Guzzi Plepis, D.K. Das-Gupta, Anionic collagen: polymer composites with improved dielectric and rheological properties, *Artif. Organs* 22 (1998) 203–209, <https://doi.org/10.1046/j.1525-1594.1998.06109.x>.
- [45] J. Steinhaus, B. Hausnerova, T. Haenel, M. Großgarten, B. Möglinger, Curing kinetics of visible light curing dental resin composites investigated by dielectric analysis (DEA), *Dent. Mater.* 30 (2014) 372–380, <https://doi.org/10.1016/j.dental.2013.12.013>.
- [46] K. Xu, W. Sun, Y. Shao, F. Wei, X. Zhang, W. Wang, P. Li, Recent development of PeakForce Tapping mode atomic force microscopy and its applications on nanoscience, *Nanotechnol. Rev.* 7 (2018) 605–621, <https://doi.org/10.1515/ntrev-2018-0086>.
- [47] D. Deng, H. Yang, J. Guo, X. Chen, W. Zhang, C. Huang, Effects of different artificial ageing methods on the degradation of adhesive–dentine interfaces, *J. Dent.* 42 (2014) 1577–1585, <https://doi.org/10.1016/j.jdent.2014.09.010>.
- [48] K. Li, H. Yang, H. Yan, Y. Sun, X. Chen, J. Guo, J. Yue, C. Huang, Quercetin as a simple but versatile primer in dentin bonding, *RSC Adv.* 7 (2017) 36392–36402, <https://doi.org/10.1039/c7ra07467k>.
- [49] H. Yang, K. Li, H. Yan, S. Liu, Y. Wang, C. Huang, High-performance therapeutic quercetin-doped adhesive for adhesive–dentin interfaces, *Sci. Rep.* 7 (2017) 1–11, <https://doi.org/10.1038/s41598-017-08633-3>.
- [50] K. Li, Z. Zhang, Y. Sun, H. Yang, J.K.H. Tsoi, C. Huang, C.K.Y. Yiu, In vitro evaluation of the anti-proteolytic and cross-linking effect of mussel-inspired monomer on the demineralized dentin matrix, *J. Dent.* 111 (2021) 103720, <https://doi.org/10.1016/j.jdent.2021.103720>.
- [51] A.F. Montagner, R. Sarkis-Onofre, T. Pereira-Cenci, M.S. Cenci, MMP inhibitors on dentin stability: a systematic review and meta-analysis, *J. Dent. Res.* 93 (2014) 733–743, <https://doi.org/10.1177/0022034514538046>.
- [52] M. Tauro, A. Laghezza, F. Loiodice, L. Piemontese, A. Caradonna, D. Capelli, R. Montanari, G. Pochetti, A. Di Pizio, M. Agamennone, C. Campestre, P. Tortorella, Catechol-based matrix metalloproteinase inhibitors with additional antioxidative activity, *J. Enzym. Inhib. Med. Chem.* 31 (2016) 25–37, <https://doi.org/10.1080/14756366.2016.1217853>.
- [53] C.E. Brubaker, H. Kissler, L.J. Wang, D.B. Kaufman, P.B. Messersmith, Biological performance of mussel-inspired adhesive in extrahepatic islet transplantation, *Biomaterials* 31 (2010) 420–427, <https://doi.org/10.1016/j.biomaterials.2009.09.062>.
- [54] G. Bilic, C. Brubaker, P.B. Messersmith, A.S. Mallik, T.M. Quinn, C. Haller, E. Done, L. Gucciardo, S.M. Zeisberger, R. Zimmermann, J. Deprest, A.H. Zisch, Injectable candidate sealants for fetal membrane repair: bonding and toxicity in vitro, *Am. J. Obstet. Gynecol.* 202 (2010), <https://doi.org/10.1016/j.ajog.2009.07.051>, 85.e1–9.
- [55] M. Nurunnabi, Z. Khatun, M. Nafuijjan, D.G. Lee, Y.K. Lee, Surface coating of graphene quantum dots using mussel-inspired polydopamine for biomedical optical imaging, *ACS Appl. Mater. Interfaces* 5 (2013) 8246–8253, <https://doi.org/10.1021/am4023863>.
- [56] Y. Dai, D. Yang, D. Yu, C. Cao, Q. Wang, S. Xie, L. Shen, W. Feng, F. Li, Mussel-inspired polydopamine-coated lanthanide nanoparticles for NIR-II/CT dual imaging and photothermal therapy, *ACS Appl. Mater. Interfaces* 9 (2017) 26674–26683, <https://doi.org/10.1021/acsami.7b06109>.
- [57] Y. Dang, M. Quan, C.M. Xing, Y.B. Wang, Y.K. Gong, Biocompatible and antifouling coating of cell membrane phosphorylcholine and mussel catechol modified multi-arm PEGs, *J. Mater. Chem. B* 3 (2015) 2350–2361, <https://doi.org/10.1039/c4tb02140a>.
- [58] H. Qi, W. Zheng, X. Zhou, C. Zhang, L. Zhang, A mussel-inspired chimeric protein as a novel facile antifouling coating, *Chem. Commun.* 54 (2018) 11328–11331, <https://doi.org/10.1039/c8cc05298k>.
- [59] Z. Tang, M. Zhao, Y. Wang, W. Zhang, M. Zhang, H. Xiao, L. Huang, L. Chen, X. Ouyang, H. Zeng, H. Wu, Mussel-inspired cellulose-based adhesive with biocompatibility and strong mechanical strength via metal coordination, *Int. J. Biol. Macromol.* 144 (2020) 127–134, <https://doi.org/10.1016/j.ijbiomac.2019.12.076>.
- [60] W. Zhu, J. Yang, J. Iqbal, Y. Peck, C. Fan, D.A. Wang, A mussel-inspired double-crosslinked tissue adhesive on rat mastectomy model: seroma prevention and in vivo biocompatibility, *J. Surg. Res.* 215 (2017) 173–182, <https://doi.org/10.1016/j.jss.2017.03.020>.
- [61] L. Huang, Y.H. Xiao, X.D. Xing, F. Li, S. Ma, L.L. Qi, J.H. Chen, Antibacterial activity and cytotoxicity of two novel cross-linking antibacterial monomers on oral pathogens, *Arch. Oral Biol.* 56 (2011) 367–373, <https://doi.org/10.1016/j.archoralbio.2010.10.011>.
- [62] K. Li, J.K.H. Tsoi, C.K.Y. Yiu, The application of novel mussel-inspired compounds in dentistry, *Dent. Mater.* 37 (2021) 655–671, <https://doi.org/10.1016/j.dental.2021.01.005>.